Implications of earthquake focal mechanisms for the frictional strength of the San Andreas fault system

JOHN TOWNEND & MARK D. ZOBACK
Department of Geophysics, Stanford University, Stanford, CA 94305-2215, USA
(e-mail: jtownend@stanford.edu)

Abstract: Analysis of stress orientation data from earthquake focal plane mechanisms adjacent to the San Andreas fault in the San Francisco Bay area and throughout southern California indicates that the San Andreas fault has low frictional strength. In both regions, available stress orientation data indicate low levels of shear stress on planes parallel to the San Andreas fault. In the San Francisco Bay area, focal plane mechanisms from within 5 km of the San Andreas and Calaveras fault zones indicate a direction of maximum horizontal compression nearly orthogonal to both subvertical, right-lateral strike-slip faults, a result consistent with those obtained previously from studies of aftershocks of the 1989 Loma Prieta earthquake. In southern California, the direction of maximum horizontal stress near the San Andreas fault is nearly everywhere at a high angle to it, similarly indicating that the fault has low frictional strength. Thus, along these two major sections of the San Andreas fault (which produced great earthquakes in southern California in 1857 and central and northern California in 1906), the frictional strength of the fault is much lower than expected for virtually any common rock type if near-hydrostatic pore pressure exists at depth, and so low as to produce no discernible shear-heating anomaly.

Our findings in southern California are in marked contrast to recent suggestions by Hardebeck & Hauksson that stress orientations rotate systematically within *c.* 25 km of the fault, which prompted a high frictional strength model of the San Andreas fault. As we utilize the same stress data and inversion technique as Hardebeck & Hauksson, we interpret the difference in our findings as being related to the way in which we group focal plane mechanisms to find the best-fitting stress tensor. We suggest that the Hardebeck & Hauksson gridding scheme may not be consistent with the requisite *a priori* assumption of stress homogeneity for each set of earthquakes.

Finally, we find no evidence of regional stress changes associated with the occurrence of the 1992 M7.4 Landers earthquake, again in apparent contradiction with the findings of Hardebeck & Hauksson.

Although it is well known that the San Andreas fault (SAF) system (Fig. 1) has been the locus of prolonged, localized deformation in the lithosphere separating the Pacific and North American plates for several million years, the level of shear stress required to cause the major faults of the San Andreas system to slip during earthquakes in the seismogenic upper *c.* 15 km of the crust remains controversial (Lachenbruch & McGarr 1990). Specifically, although laboratory experiments systematically reveal coefficients of friction of between 0.6 and 1.0 (Byerlee 1978), consistent with stress levels measured to depths of several kilometres in intraplate regions (Townend & Zoback 2000) two lines of evidence suggest that coefficients of friction, μ, along the major faults of the San Andreas system are substantially lower. First, heat flow data reveal that the surface trace of the SAF is not associated with the marked, positive thermal anomaly expected if the coefficient of friction were any higher than 0.2 (Brune *et al.* 1969; Lachenbruch & Sass 1980, 1992; Lachenbruch & McGarr 1990). Second, measurements of principal stress directions along the SAF suggest that the angle between the greatest compressive stress direction and the fault plane almost invariably exceeds the directions expected for $0.6 \leqslant \mu \leqslant 1.0$ ('hydrostatic Byerlee's law'; Brace & Kohlstedt 1980; Townend & Zoback 2000) and, in fact, locally exceeds 80° at several locations (Mount & Suppe 1987; Zoback *et al.* 1987; Jones 1988; Oppenheimer *et al.* 1988; Zoback & Beroza 1993). Such high angles of compression imply friction coefficients of <0.1 (Lachenbruch &

From: HOLDSWORTH, R.E., STRACHAN, R.A., MAGLOUGHLIN, J.F. & KNIPE, R.J. (eds) 2001. *The Nature and Tectonic Significance of Fault Zone Weakening*. Geological Society, London, Special Publications, **186**, 13–21. 0305-8719/01/$15.00

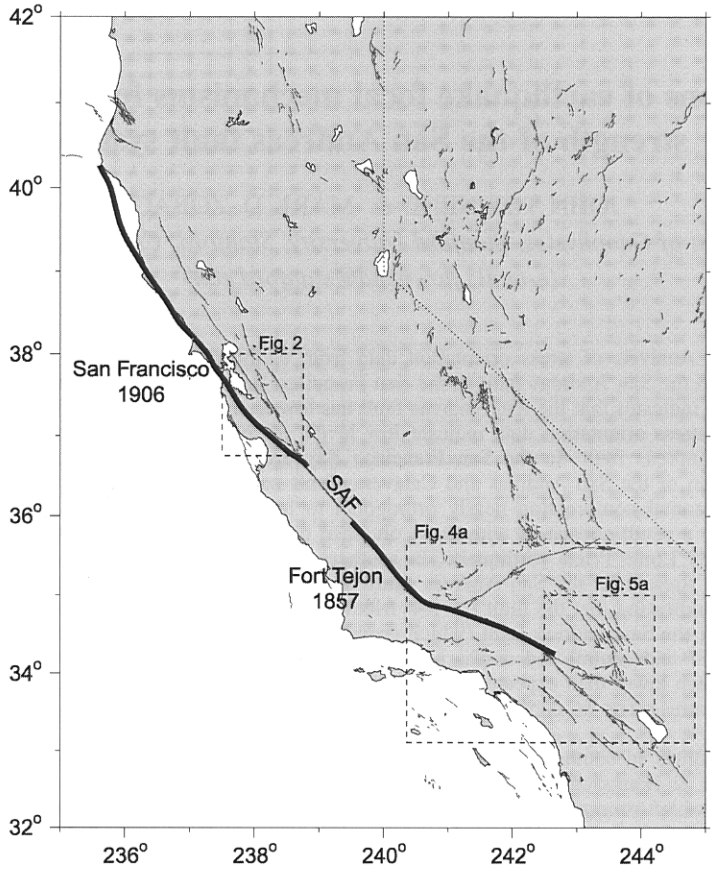

Fig. 1. Map of California illustrating the San Andreas fault (SAF) and other major faults. The thick lines along sections of the San Andreas fault indicate those portions of the fault that ruptured during the 1857 Fort Tejon and 1906 San Francisco earthquakes. The areas corresponding to Figs. 2, 4a and 5a are shown by the dashed boxes.

Sass 1992) or high fluid pressures within the fault zone (Rice 1992).

Hardebeck & Hauksson (1999) recently suggested that whereas the far-field axis of greatest horizontal compression, $S_{H\max}$, is at a high angle to the average strike of the SAF throughout much of southern California, the stress tensor rotates systematically adjacent to the fault so that the relevant near-field angle is *c.* 45°. Further, it was suggested that this behaviour is particularly pronounced in the vicinity of the 'Big Bend' area near Fort Tejon. This led Scholz (2000) to postulate a mechanical model of the SAF in which the fault is strong and stress rotation is a direct consequence of frictionless slip below the locked zone.

In this paper we use well-located earthquake focal mechanisms to infer principal stress orientations in the vicinity of the San Andreas fault system in the San Francisco Bay area and in southern California (Fig. 1). Our primary aim is to determine the orientation of $S_{H\max}$ close to the SAF and adjacent faults, where 'close' denotes a distance less than the thickness of seismogenic crust (*c.* 10–15 km). In the San Francisco Bay area we have compiled previous workers' results and obtained an additional stress orientation result by focal mechanism inversion. With the analysis of the southern California data our motivation is to repeat the analysis of Hardebeck & Hauksson (1999) with the specific objective of investigating the influence of their gridding scheme. In other words, we wish to address the method with which they grouped focal mechanism data to determine stress orientations.

The fundamental basis for inverting a group of fault slip observations or focal mechanisms to infer stress orientations is the assumption that slip in each event occurred within a uniform stress field (Angelier 1979, 1984; Gephart & Forsyth 1984; Michael 1984, 1987). Hardebeck

& Hauksson (1999) used rectangular 'boxes' when selecting focal mechanisms for inversion to examine stress orientation as a function of distance from the San Andreas fault. The dimensions of these boxes varied greatly, from as little as 25 km and 2 km in the local strike-parallel and strike-perpendicular directions, respectively, to more than 150 km and 60 km. Along the Fort Tejon profile, on which the model of Scholz (2000) was subsequently based, the strike-parallel length of the boxes is 80 km: consequently, focal mechanisms separated by as much as *c.* 80 km were combined into boxes for inversion. Given that the SAF exhibits a *c.* 25° change of strike in the Fort Tejon area and intersects the left-lateral Garlock fault, stress is unlikely to be homogeneous on 80 km scales, and it may be inappropriate to group such widely separated focal mechanisms. In effect, the gridding scheme used by Hardebeck & Hauksson may not be consistent with the *a priori* assumption of stress homogeneity within each group of earthquakes.

Finally, using the southern California dataset we wish to examine the possibility of stress changes induced by the 1992m M7.4 Landers earthquake. Hardebeck & Hauksson (1999) reported an apparent clockwise stress rotation of as much as 40° caused by this earthquake. If that were the case, it would indicate that the stress changes associated with this earthquake were of comparable magnitude to tectonic stress levels. As average earthquake stress drops (determined seismologically) of 1–10 MPa (Kanamori & Anderson 1975) are small relative to crustal stress levels consistent with hydrostatic Byerlee's law, any such stress rotations would imply that the crust, as well as major faults, had low frictional strength.

San Francisco Bay area

Four major SSE–NNW-striking faults, the San Gregorio, San Andreas, Hayward and Calaveras faults (Fig. 2) accommodate varying amounts of right-lateral slip and relative plate motion in the San Francisco Bay area. San Francisco Bay itself, bounded to the SW and NE by the San Francisco Peninsula Ranges and Diablo Ranges–East Bay Hills, respectively, is relatively aseismic, but microseismicity levels are high along each of the principal fault strands, and the region has experienced several major historic earthquakes. Notable 20th-century events include the 1906 M7.8 San Francisco and 1989 M6.9 Loma Prieta earthquakes on the SAF and the 1984 M6.2 Morgan Hill earthquake on the Calaveras fault.

Previous studies using focal mechanisms of aftershocks following the Morgan Hill and Loma Prieta events have revealed stress orientations in which the angles between $S_{H\max}$ and the local fault strike are 80–90° (Oppenheimer *et al.* 1988; Zoback & Beroza 1993). We have supplemented these two results with one other obtained for a suite of 28 earthquakes that occurred on the southern San Francisco Peninsula (the area encompassed by the box along the SAF west of San Jose in Fig. 2) between 1970 and 1999 (Zoback *et al.* 1999). These earthquakes are a subset of those shown in cross-section in Fig. 3a: they occurred on either side of the quiescent SAF and exhibited a mixture of reverse and strike-slip focal mechanisms. We have used the inversion algorithm of Gephart & Forsyth (1984) and Gephart (1990*a*, *b*) to determine an optimal stress tensor that minimizes the one-norm misfit between the observed and calculated shear tractions on either of the two nodal planes in each focal mechanism. Not unexpectedly, the inversion indicates a strike-slip–reverse faulting regime in which the intermediate and least principal stresses have approximately the same magnitude. The best-fitting solution is illustrated in Fig. 3b: the trend and plunge of S_1, which is $S_{H\max}$ in this case, are 221° and 6°, respectively. S_2 and S_3 (the vertical stress) trend 130° and 334°, and plunge 14° and 75°, respectively. The average misfit of the optimal solution for the 28 focal mechanisms is 4.9°. It is clear from these results that near fault-normal compressive stress exists in the seismogenic crust immediately adjacent to the SAF.

This finding is similar to that of Oppenheimer *et al.* (1988), who studied aftershocks of the 1984 Morgan Hill earthquake. A precise relocation of these events is shown in Fig. 3c (Schaff, pers. comm.). Thrust events on planes parallel to the Calaveras fault and strike-slip events on north–south-trending faults are observed adjacent to the right-lateral, strike-slip Calaveras fault. As in the case of the events along the SAF, Oppenheimer *et al.* (1988) found a best-fitting stress tensor for which $S_{H\max}$ was essentially perpendicular to the trend of the Calaveras fault (Fig. 3d). These results, combined with those of Zoback & Beroza (1993) for the diverse aftershock focal plane mechanisms of the Loma Prieta earthquake (Fig. 2), make a convincing case that $S_{H\max}$ orientations are consistently at an angle of >80° to the local strike of the San Andreas or Calaveras faults. Importantly, the stress orientation estimates in each case are indicative of conditions within 5–

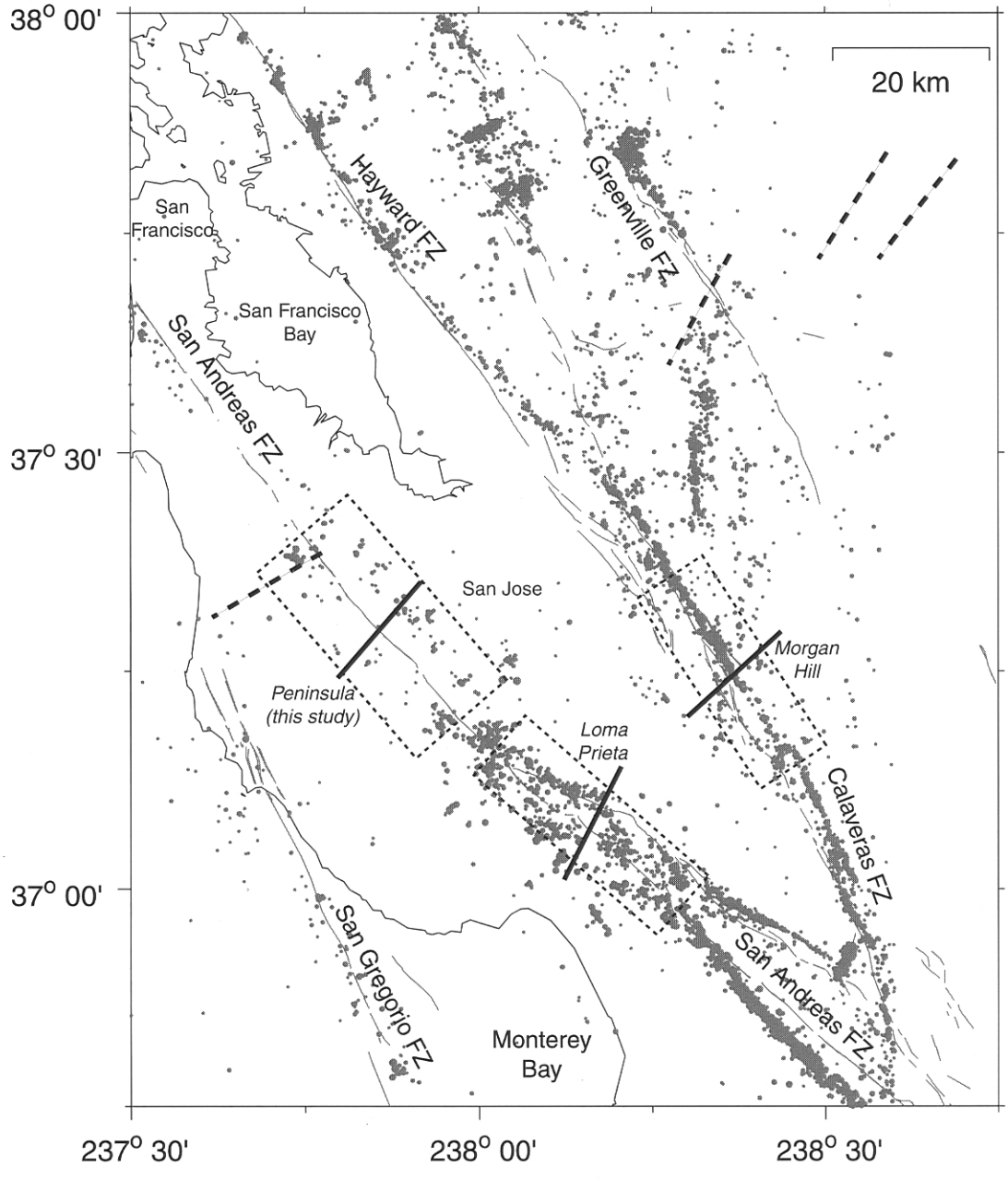

Fig. 2. Map of the San Francisco Bay area showing the orientation of $S_{H\max}$ obtained by focal mechanism inversion (continuous lines) and borehole breakout analysis (dashed lines). The dotted rectangles centred on the three focal mechanism results illustrate the spatial distribution of focal mechanisms used in the 1984 Morgan Hill (Oppenheimer *et al.* 1988), 1991 Loma Prieta (Zoback & Beroza 1993), and southern San Francisco Peninsula (this study) stress inversions. The dots indicate seismicity larger than M2 between 1965 and 2000. Historic and Holocene fault data courtesy of the California Department of Mines and Geology.

10 km of the respective faults, thus indicating fault-normal compressive stress within the crustal volumes adjacent to the seismogenic sections of the San Andreas and Calaveras faults. Four $S_{H\max}$ estimates obtained from borehole breakout data and shown in Fig. 2 reinforce the picture of fault normal compression in the San Francisco Bay area. That both the San Andreas

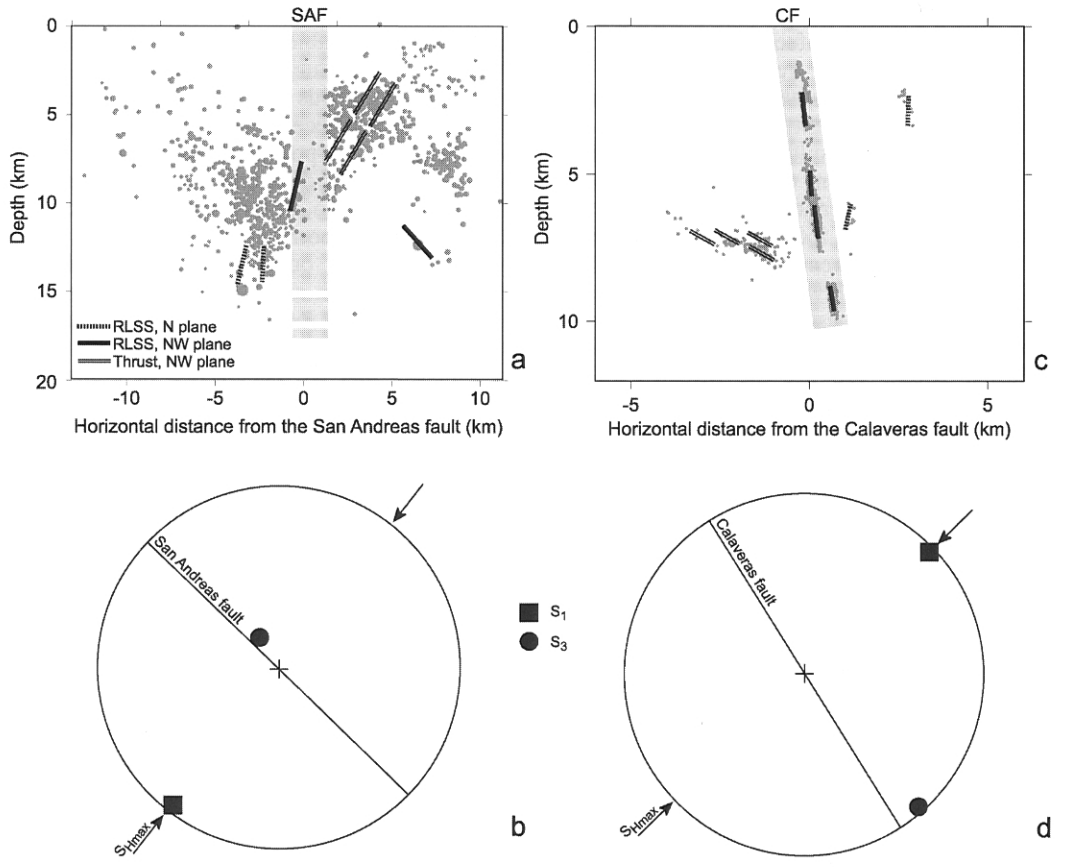

Fig. 3. (**a**) Cross-section across the San Andreas fault on the southern San Francisco Peninsula, west of San Jose, illustrating the distribution of near-fault seismicity (M1.5 and greater). The data have been projected onto a plane orthogonal to the SAF. RLSS, right lateral strike-slip. Data and geological interpretations from Zoback *et al.* (1999). (**b**) Optimal stress tensor obtained by inversion of focal mechanisms for 28 earthquakes larger than M3; the locations of the earthquakes lie within the upper rectangle centred on the San Andreas fault in Fig. 2. S_1 and S_3 are axes of greatest and least compressive stress, respectively. Data from Zoback *et al.* (1999). (**c**) Cross-section across the Calaveras fault (CF) in the vicinity of the 1984 Morgan Hill earthquake. Hypocentral data and fault interpretation courtesy of Schaff (pers. comm.). (**d**) Preferred stress tensor obtained by Oppenheimer *et al.* (1988) for the Morgan Hill aftershock sequence.

and Calaveras faults are able to slip under near-field fault-normal compression indicates that they are very weak with respect to hydrostatic Byerlee's law.

Stress in southern California

As alluded to above, the gridding method of Hardebeck & Hauksson (1999) results in widely separated focal mechanisms being combined for stress inversion. The essential limitation of this method is that it takes no account of either structural trends (other than the average strike of the SAF) or data clustering. To determine whether their grid design adversely affects stress inversion results in southern California, we have opted to use a recursive quadtree algorithm to grid the data. Starting from a single square box encompassing all the earthquake locations, the algorithm operates by dividing the box into quarters and continuing recursively within each quarter until there are fewer than n_{max} earthquake locations in each box or the box reaches a minimum dimension of x_{min}. The latter condition is a modification of the standard quadtree algorithm that we have incorporated to avoid boxes that are smaller than errors in the earthquake locations. The resultant grid comprises an irregular mesh of square boxes that are smaller and more densely spaced in areas containing many earthquakes. In practice, we impose an additional condition that restricts the

stress inversion to those boxes containing more than n_{min} events. We feel that this gridding scheme is geologically reasonable because it combines earthquakes within contiguous crustal volumes of limited extent.

To compare our results directly to those of Hardebeck & Hauksson, we have used the same dataset and stress inversion method. The dataset contains first-motion focal mechanisms for *c.* 49 000 earthquakes recorded by the southern California seismic network between 1981 and 1999 and relocated using a three-dimensional velocity model (Hardebeck & Hauksson 1999; Hauksson 2000). We use the Michael (1984, 1987) stress inversion method with equal weighting for both nodal planes.

Figure 4a illustrates the results for southern California obtained by inverting the entire dataset after gridding with the parameters $n_{min} = 30$, $n_{max} = 100$, and $x_{min} = 5$ km. It should be noted that this procedure produces square boxes of *c.* 5.6 km width in regions of dense seismicity, such as the vicinities of the Northridge and Landers earthquakes (denoted by N and L, respectively) and boxes of 5.6–22 km width along the SAF. Within the Mojave Desert, the triangular fault-bounded region in the middle of Fig. 4, the average box size is *c.* 44 km, reflecting the relatively sparse seismicity. We are confident that the gridding technique is robust because the $S_{H\max}$ orientations in adjacent boxes are very similar despite each actual focal mechanism inversion being independent of those surrounding it.

In general, $S_{H\max}$ trends slightly east of north and is oriented at a high angle to the fault strike of each major fault strand illustrated. Figures 4b and c illustrate the near-field stress orientation data (those data points closer than 5 km to the fault trace) along the San Andreas fault. The mean and standard deviation of the angle between $S_{H\max}$ and the local fault strike are 64° and 14°, respectively, indicating that the near-field angle is significantly different at the 95% level of confidence from that suggested by Hardebeck & Hauksson (1999) for some of their profiles and later utilized by Scholz (2000) to argue for a strong San Andreas fault. This result agrees, however, with that of Jones (1988), who found that the mean angle exceeded 60°. Contrary to Hardebeck & Hauksson (1999), we do not observe a consistent pattern of stress rotation close to either the SAF or the other major faults.

We have also investigated the effect of the 1992 Landers earthquake on the local stress field. Using a relatively simple approach, we have inverted the focal mechanisms before and after this event separately to determine whether or not any detectable stress rotation is evident (Fig. 5a). The nature of the quadtree algorithm means that the grids corresponding to different datasets are not necessarily the same, implying that the pre- and post-earthquake stress inversions are made at different locations. We have compared the two datasets only at locations <5 km apart. The comparisons were made separately inside and outside the zones of pronounced aftershock activity (defined by areas of aftershock activity occurring within 30 days of the main shock). This distinction is made on the presumption that the occurrence of aftershocks (the 'aftershock zone') implies a possibly significant stress perturbation, whereas a lack of aftershock activity implies no significant earthquake-induced change. Thus, the latter case constitutes a control zone in which we expect to observe no rotation if the technique is appropriate.

It is qualitatively apparent from Fig. 5a that there is little systematic difference in the pre- and post-Landers stress orientations. This observation is substantiated in Fig. 5b and c, in which the differences in orientation in the control zone (mean −0.8°; SD 12.2°; 46 observations) and aftershock zone (mean 1.4°; SD 12.7°; 19 observations) are compared. Neither of these samples is significantly different from zero at the 95% level of confidence. Both standard deviations are similar to those obtained for the southern California dataset as a whole, and suggest that small earthquake-induced rotations are unlikely to be observed given the stress uncertainties.

Discussion

The data from both the San Francisco Bay area and southern California reveal high angles between the local fault strike and the direction of maximum horizontal compression. Indeed, this observation applies both to the SAF and associated faults, and suggests that weakness is characteristic of these portions of the North America–Pacific plate boundary.

The discrepancies between our southern California results and those of Hardebeck & Hauksson (1999) must stem from the different gridding methods used, as the dataset and focal mechanism inversion procedures were the same. By using an iterative gridding algorithm that incorporates spatial variations in seismicity, it has been possible to obtain a high-resolution image of near-fault stress orientations (where justified by the data) without needlessly com-

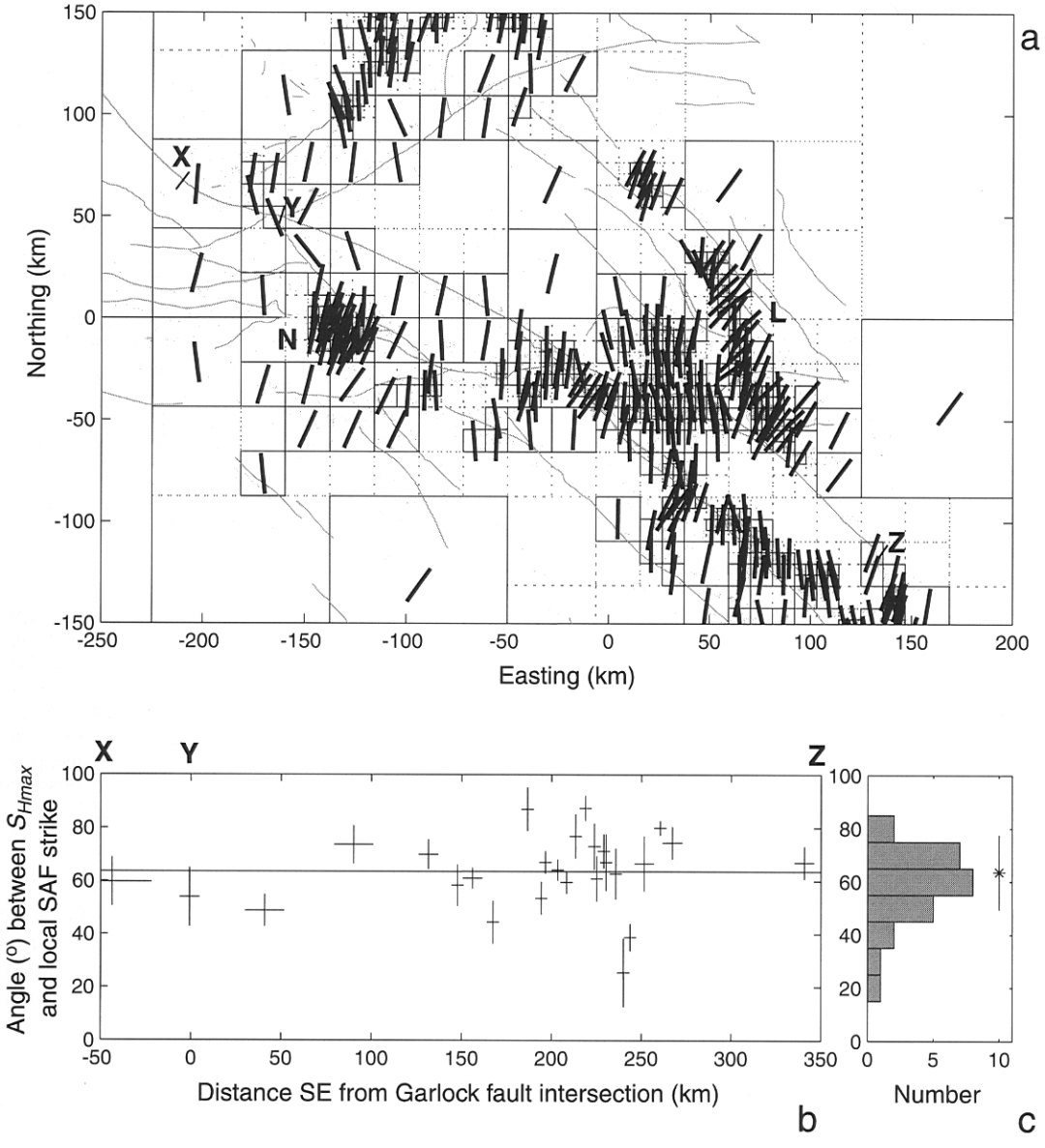

Fig. 4. (**a**) $S_{H\max}$ orientation results obtained using the quadtree gridding algorithm and the Michael (1994, 1987) stress inversion routine for the 1981–1999 M1+ southern California dataset utilized by Hardebeck & Hauksson (1999). Boxes containing <30 focal mechanisms are dashed, and no inversion was made at those locations. L, N, areas of seismicity associated with the 1992 Landers and 1994 Northridge earthquakes, respectively; X, Y, Z, trace of the San Andreas fault profile illustrated in (**b**). (**b**) Along-fault profile (X–Y–Z) of the angle between near-field $S_{H\max}$ estimates (lying within 5 km of the San Andreas fault trace) and the local fault strike. The horizontal error bars indicate the width of the box used for each inversion, and the vertical error bars indicate the 95% confidence bounds estimated by bootstrap analysis. The mean of all estimates (64°) is indicated by the continuous horizontal line. (**c**) Histogram of the data shown in (**b**). The mean and standard deviation (14°) are indicated by the star and vertical error bars, respectively.

promising the assumption of local stress homogeneity. Our results are incompatible with the model of Scholz (2000), which predicts symmetric rotation about the SAF over lateral distances of ± 20 km. We have particularly strong reservations about the applicability of a 2D plane-strain model to a segment of the SAF that is clearly curved and, moreover, intersects

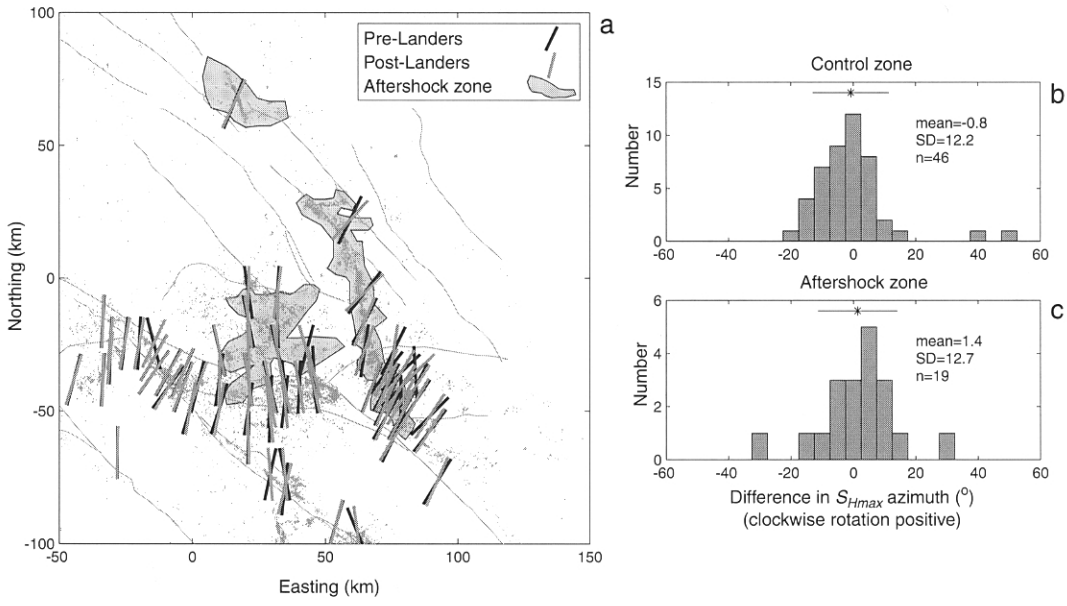

Fig. 5. (**a**) $S_{H\max}$ orientations before (black) and after (grey) the Landers 1992 earthquake. The gridding parameters for each inversion are the same as in Fig. 4a, but the resultant grids are different before and after the earthquake, and are not shown. The light grey shaded regions indicate regions of aftershocks (see text for details). (**b**) Histogram of differences in pre- and post-Landers stress orientations outside the zones of aftershock activity. The values plotted are the post-Landers orientation minus the pre-Landers orientation; clockwise rotations are positive. The mean (−0.8°) and standard deviation (12.2°) of the 46 data points are illustrated by the star and horizontal error bar, respectively. (**c**) Histogram of differences in pre- and post-Landers stress orientations within the aftershock zone. No significant change in stress orientation is observed in either the control zone or the aftershock zone.

another large fault. It is noteworthy that the only data presented by Hardebeck & Hauksson (1999) that are satisfactorily fitted by the Scholz model are those from the complex 'Big Bend' area.

The significance of our results is that any postulated stress rotation must occur within a zone no more than several kilometres wide, centred on the fault zone, or otherwise it would be detectable. Any such zone must be narrow, on theoretical grounds, or the fluid pressure would overcome the least principal stress and hydrofracture the surrounding crust (Rice 1992). As pointed out by Scholz (2000), the 20–30 km wide zone of stress rotation suggested by Hardebeck & Hauksson (1999) is inconsistent with the Rice (1992) model of a high-pressure fault core. Although our data do not possess sufficient resolution to observe stress rotations on the scale of *c.* 1 km, it is clear that within ±5 km of the SAF $S_{H\max}$ is at a much higher angle to the fault than is consistent with conventional Coulomb faulting and hydrostatic Byerlee's law. In other words, these data clearly illustrate that the fault has low frictional strength.

Conclusions

We have compiled stress orientation data in the San Francisco Bay area and reanalysed stress orientations in southern California using focal mechanism data. In the San Francisco Bay area, focal mechanism stress inversions indicate that the maximum horizontal compressive stress is oriented almost orthogonally to the strikes of the San Andreas and Calaveras faults. Using the same dataset and inversion method as Hardebeck & Hauksson (1999) we have demonstrated that their postulated near-fault stress rotation may be an artefact of combining widely separated focal mechanisms into single inversions. Using a geologically reasonable and mathematically more sophisticated gridding algorithm that takes into account spatial clustering of seismicity, we have been able to obtain stress orientations while justifying to the extent that the data warrant the necessary assumption of stress homogeneity within contiguous crustal blocks. Furthermore, applying this technique to the 1992 Landers earthquake reveals no consistent differences in stress orientation before and after the main shock.

Overall, available stress orientation results from the San Francisco Bay area and southern California strongly indicate low levels of shear stress on planes parallel to the San Andreas fault. In the San Francisco Bay area, several data are available within ± 5 km of the main fault zone that indicate a direction of maximum horizontal compression nearly orthogonal to the San Andreas and Calaveras faults, and the fault that produced the Loma Prieta earthquake. In southern California, the direction of maximum horizontal stress near the San Andreas fault is generally at a high angle to it (averaging >60°), similarly indicating that the fault has low frictional strength.

We are grateful to D. Schaff and G. Beroza of Stanford University for making their Calaveras fault earthquake relocation data available, S. Prejean of Stanford University for valuable suggestions, M. L. Zoback for the San Francisco Peninsula seismicity data, and to D. Cowan and P. Sammonds for considerate reviews. Fault data courtesy of the California Department of Mines and Geology. This work was supported by the National Science Foundation (award 96-14267) and an Arco Stanford Graduate Fellowship (to J.T.).

References

ANGELIER, J. 1979. Determination of the mean principal directions of stresses for a given fault population. *Tectonophysics*, **56**, T17–T26.

ANGELIER, J. 1984. Tectonic analysis of fault slip data sets. *Journal of Geophysical Research*, **89**, 5835–5848.

BRACE, W.F. & KOHLSTEDT, D. 1980. Limits on lithospheric stress imposed by laboratory measurements. *Journal of Geophysical Research*, **85**, 6248–6252.

BRUNE, J.N., HENYEY, T.L. & ROY, R.F. 1969. Heat flow, stress, and rate of slip along the San Andreas fault, California. *Journal of Geophysical Research*, **74**, 3821–3827.

BYERLEE, J.D. 1978. Friction of rocks. *Pure and Applied Geophysics*, **116**, 615–626.

GEPHART, J.W. 1990*a*. Stress and the direction of slip on fault planes. *Tectonics*, **9**, 845–858.

GEPHART, J.W. 1990*b*. FMSI: A Fortran program for inverting fault/slickenside and earthquake focal mechanism data to obtain the regional stress tensor. *Computers and Geosciences*, **16**, 953–989.

GEPHART, J.W. & FORSYTH, D.W. 1984. An improved method for determining the regional stress tensor using earthquake focal mechanism data: application to the San Fernando earthquake sequence. *Journal of Geophysical Research*, **89**, 9305–9320.

HARDEBECK, J.L. & HAUKSSON, E. 1999. Role of fluids in faulting inferred from stress field signatures. *Science*, **285**, 236–239.

HAUKSSON, E. 2000. Crustal structure and seismicity distributions adjacent to the Pacific and North America plate boundary in southern California. *Journal of Geophysical Research*, **105**, 13875–13903.

JONES, L.M. 1988. Focal mechanisms and the state of stress on the San Andreas fault in southern California. *Journal of Geophysical Research*, **93**, 8869–8891.

KANAMORI, H. & ANDERSON, D.L. 1975. Theoretical basis of some empirical relations in seismology. *Bulletin of the Seismological Society of America*, **65**, 1073–1095.

LACHENBRUCH, A.H. & MCGARR, A. 1990. Stress and heat flow. *US Geological Survey Professional Paper*, **1515**, 261–277.

LACHENBRUCH, A.H. & SASS, J.H. 1980. Heat flow and energetics of the San Andreas fault zone. *Journal of Geophysical Research*, **85**, 6185–6223.

LACHENBRUCH, A.H. & SASS, J.H. 1992. Heat flow from the Cajon Pass, fault strength, and tectonic implications. *Journal of Geophysical Research*, **97**, 4995–5015.

MICHAEL, A.J. 1984. Determination of stress from slip data: faults and folds. *Journal of Geophysical Research*, **89**, 11517–11526.

MICHAEL, A.J. 1987. Use of focal mechanisms to determine stress: a control study. *Journal of Geophysical Research*, **92**, 357–368.

MOUNT, V.S. & SUPPE, J. 1987. State of stress near the San Andreas fault: implications for wrench tectonics. *Geology*, **15**, 1143–1146.

OPPENHEIMER, D.H., REASENBERG, P.A. & SIMPSON, R.W. 1988. Fault plane solutions for the 1984 Morgan Hill, California, earthquake sequence: evidence for the state of stress on the Calaveras fault. *Journal of Geophysical Research*, **93**, 9007–9026.

RICE, J.R. 1992. Fault stress states, pore pressure distributions, and the weakness of the San Andreas fault. *In*: EVANS, B. & WONG, T.F. (eds) *Fault Mechanics and Transport Properties of Rocks*. Academic Press, New York, 475–503.

SCHOLZ, C.H. 2000. Evidence for a strong San Andreas fault. *Geology*, **28**, 163–166.

TOWNEND, J. & ZOBACK, M.D. 2000. How faulting keeps the crust strong. *Geology*, **28**, 399–402.

ZOBACK, M.D. & BEROZA, G.C. 1993. Evidence for near-frictionless faulting in the 1989 (M6.9) Loma Prieta, California, earthquake and its aftershocks. *Geology*, **21**, 181–185.

ZOBACK, M.D., ZOBACK, M.L., MOUNT, V.S. & 20 OTHERS 1987. New evidence for the state of stress of the San Andreas fault system. *Science*, **238**, 1105–1111.

ZOBACK, M.L., JACHENS, R.C. & OLSON, J.A. 1999. Abrupt along-strike change in tectonic style: San Andreas fault zone, San Francisco Peninsula. *Journal of Geophysical Research*, **104**, 10719–10742.